



HAL
open science

Thermo-physical properties measurements of hygroscopic and reactive material (zeolite 13X) for open adsorptive heat storage operation

Elliot Sculler, Patrick Dutournié, Mohamed Zbair, Simona Bennici

► **To cite this version:**

Elliot Sculler, Patrick Dutournié, Mohamed Zbair, Simona Bennici. Thermo-physical properties measurements of hygroscopic and reactive material (zeolite 13X) for open adsorptive heat storage operation. *Journal of Thermal Analysis and Calorimetry*, 2022, 147 (22), pp.12409-12416. 10.1007/s10973-022-11439-9 . hal-03856161

HAL Id: hal-03856161

<https://hal.science/hal-03856161v1>

Submitted on 16 Nov 2022

HAL is a multi-disciplinary open access archive for the deposit and dissemination of scientific research documents, whether they are published or not. The documents may come from teaching and research institutions in France or abroad, or from public or private research centers.

L'archive ouverte pluridisciplinaire **HAL**, est destinée au dépôt et à la diffusion de documents scientifiques de niveau recherche, publiés ou non, émanant des établissements d'enseignement et de recherche français ou étrangers, des laboratoires publics ou privés.

Thermo-physical properties measurements of hygroscopic and reactive material (zeolite 13X) for open adsorptive heat storage operation

Elliot Scuille^{1,2,3}, Patrick Dutournié^{1,2*}, Mohamed Zbair^{1,2}, Simona Bennici^{1,2}

¹ Université de Haute-alsace, CNRS, IS2M UMR 7361, 3 rue Alfred Werner 68093 Mulhouse Cedex, France

² Université de Strasbourg, France

³ Réseaux de Chaleur Urbains d'Alsace, 14 place des halles, 67000 Strasbourg, France

* Corresponding author details: patrick.dutournie@uha.fr

Abstract:

The determination of the thermo-physical properties (density, specific heat capacity, and thermal conductivity) of hygroscopic and reactive solid materials, as those applied in sorption thermochemical heat storage systems, is not trivial. Lack of precision in the measurement and contradictory results make it difficult to enter these thermal parameters in the programs used for simulating the functioning and operating scenarios of thermochemical heat storage devices. For this reason, different techniques have been applied and compared in order to improve the accuracy of the measurement. In particular, there was a difference in thermal conductivity (about 30%) between the hot disc experiments and the others, as well as a higher dispersion of the experimental data (MAD > 19%). The same was found for specific heat capacity (MAD \approx 14%). Hence, the transient hot disk method is not suitable for estimating thermal conductivity and the specific heat capacity of this type of material. Nevertheless, this technique enables a good estimation of the thermal effusivity. The thermal conductivity and the specific heat capacity were investigated by the hot wire method and by TG-DSC, respectively. A slight increase in specific heat with temperature was observed, but in the range of 70 – 95 °C, this value is constant at 913 J kg⁻¹ K⁻¹. The applied methodology was validated by comparing the experimental and calculated thermal effusivity values.

Key words: Thermo-physical properties; Heat storage; Thermal conductivity; Specific heat capacity; Zeolite 13X.

Acknowledgments: The authors would like to thank the company Thermoconcept, Mérignac, France for additional testing with transient plane source; the Association Nationale Recherche Technologie (ANRT) for the funding of this work under agreement Cifre n° 2019/0620 (E. Sculler grant); the Region Grand Est for providing funding for the acquisition of the TG-DSC equipment within the “STOCKFATAL” project; the Carnot MICA institute for funding part of this study in the frame of the STOCKENER project; IS2M for the postdoctoral grant of M. Zbair in the frame of the “Projets Structurants” call.

Declarations:**Funding**

This research was supported by the Association Nationale Recherche Technologie (ANRT) under agreement Cifre n° 2019/0620 (E. Sculler grant); the Region Grand Est (providing funding for the acquisition of the TG-DSC equipment within the “STOCKFATAL” project); the Carnot MICA institute (funding part of this study in the frame of the STOCKENER project); IS2M (postdoctoral grant of M. Zbair in the frame of the “Projets Structurants” call).

Conflicts of interest

The authors declare that they don't have any conflict of interest.

Availability of data and material

The material and the data are available upon request.

Code availability: Not applicable.

Ethics approval: Not applicable.

Consent to participate: Not applicable.

Consent for publication: Not applicable.

Authors Contribution

Conceptualization: SB and PD; methodology: SB, ES and PD, experimental work: ES, data analysis: ES, SB, MZ and PD, writing-original draft preparation: ES, SB, MZ and PD: supervision: SB and PD.

Introduction

Material characterizations are key contributions to the global development effort in the field of adsorptive heat storage and transformation [1,2]. Adsorptive heat storage cycles are based on reversible ad/desorption reactions [3,4]. Basically, the discharging phase corresponds to the adsorption of an adsorbate on an adsorbent (exothermic reaction). The major aim of this technology is to release an important amount of energy (2–3 times more than the latent heat of water) that can be stored at room temperature for a long time [5–7]. When the heat is discharged, the temperature of the material (adsorbent) is expected to increase significantly, which can damage the material and or the operating equipment. Using simulation tools has been just the safest way to minimize the risks. Indeed, a simulation program allows to test different configurations and operating conditions and can be used for scaling-up. Hong et al., [8] for example, successfully used numerical simulation to investigate the melting and solidification heat transfer characteristics in double tubes with varying numbers of fins and inner tube wall boundary conditions.

A necessary and inevitable step is to know the thermo-physical properties precisely to ensure reliable simulated results, namely the isosteric heat of adsorption, sorption equilibrium, heat capacity, bulk density, and thermal conductivity [9]. The first one is the heat generated in the material due to water adsorption [10,11]. It can be easily estimated with precision from TG-DSC investigations [12]. For the correct design and sizing in terms of heat storage and supply, it is required to know precisely the material density. The thermal inertia of a material is characterized by the product of its specific heat capacity and density. In a heat storage application for home heating, the heat supply can be significantly delayed by a variation in thermal inertia. The last one (bulk thermal conductivity of the material) manages thermal gradients in the reactor and hot points. Numerical simulations of heat and mass transfer in heat storage reactors [13,14] show significant

thermal gradients in the reactor (proportional to the bulk thermal conductivity). High temperatures can damage the material, thus degrading the operation of the heat storage system.

These different properties are functions of temperature and water content [15–17].

The material used in this application is hygroscopic and reactive, which is the main problem for the thermal properties estimation [18,19]. Indeed, most classical techniques applied to the thermal properties investigation are based on a temperature difference in the material [20]. In the present case, a change in temperature modifies the water content (sorption equilibrium) and consequently generates heat [21–23]. As pointed out by Aristov [9], a computational approach does not allow to assess thermodynamic parameters with sufficient accuracy. Direct measurement is the main alternative so far. He proposed an empirical model for the apparent specific heat capacity of the zeolite 4A–water pair [9]. Nevertheless, the respective contributions of the dry adsorbent and the adsorbed phase are not detailed. Concerning the zeolite 13X–water pair, Simonot-Grange et al. [24] measured its apparent specific heat capacity at several combinations of temperature and water content (from 16 °C to 350 °C). The results are summarized in Table 1. They reached the conclusion that the influence of adsorbed water is not negligible at low uptakes. However, data for a given temperature are limited to a single value at a single water content, and the experimental methodology appears to be worthwhile.

Table 1 Specific heat capacity of zeolite 13X from the literature

Material	$\theta/^\circ\text{C}$	$C_p \text{ dry} / \text{J kg}^{-1} \text{K}^{-1}$	$C_p \text{ hydrated} / \text{J kg}^{-1} \text{K}^{-1}$	Ref.
13X – H ₂ O	50	910	1530 ($w = 20 \text{ kg kg}^{-1}$)	[25]
13X – H ₂ O	20-350	$260+8.6 (T-273)$	1510 ($w = 26 \text{ kg kg}^{-1}$, $T = 289 \text{ K}$)	[24]

13X	40-180	$1097+3.44(T-373)$ $-0.0029 (T^2-373^2)$		[26]
13X	$\theta > 20\text{ }^\circ\text{C}$	880	$1716 + \int_{T_{min}}^T A \exp(-B(T - T_0)^2) dT$ $A = 0.03762\ B = 3.976\text{E-}4\ T_0 = 335\ \text{K}$	[27]
13X	$\theta > 20\text{ }^\circ\text{C}$	800-900		[3]

Hirasawa and Urakami [25] measured the specific heat capacity of dried zeolite 13X in the temperature range of $-50 - 50\text{ }^\circ\text{C}$. It shows a slow linear increase with temperature. They also measured the specific heat capacity of the adsorbed water. By analyzing the results, it is not obvious to confirm if the assumption that “the heat capacity of the adsorbed phase is an intermediate value between that of the gaseous state and that of the liquid state” is true [28].

The values of specific heat capacity available in the literature (Table 1) are significantly different. For example, at $\theta = 50\text{ }^\circ\text{C}$, the specific heat of dry material is 910, 690, 1026, and 880 $\text{J kg}^{-1}\ \text{K}^{-1}$, respectively, for a range of 336 $\text{J kg}^{-1}\ \text{K}^{-1}$ (relative uncertainty higher than 30%). Literature data for other materials (for example, zeolite 4A) is more consistent, but with the same variability and uncertainty [2,9,21,23,24,29].

Unlike specific heat capacity (an intrinsic property), the bulk thermal conductivity and the density are functions of the size and shape of the particles. Several studies successfully applied the “hot wire” method [15,16,18,19,30] to measure the apparent thermal conductivity of hygroscopic materials. According to Freni *et al.* [16], the temperature increasing during the transient measurement does not change the water uptake of the material [16]. In the same way, another transient method (transient plane source, also known as “hot disk”) [31] can be applied. In theory, this technique was designed to simultaneously estimate the thermal conductivity and the specific heat capacity of a material (via the thermal diffusivity and the effusivity) [32,33]. The possibility to measure several thermo-physical parameters at once with a quick procedure is appealing.

Pinheiro et al. [34] used it to measure zeolite 13X's heat conductivity in the temperature range of 25–115 °C and found it lower than $0.3 \text{ W m}^{-1} \text{ K}^{-1}$. However, the “hot disk” technique is known to face limits when applied to such low-conductivity materials [35]. This is especially the case when applied to the granular structure of the zeolite bed with a substantial void fraction. For this reason, the packing density of the bed also has to be taken into account. To the author's knowledge, few data about the zeolite 13X–water pair is available, with high variability, ranging from 76 to 400 $\text{mW m}^{-1} \text{ K}^{-1}$ [19,34,36,37]. For this reason, their values must be used with care. Thus, performing original measurements of the thermal conductivity along with the apparent density of the packed bed is relevant.

Overall, the thermophysical parameters (density, specific heat capacity, and thermal conductivity) of hygroscopic and reactive solid materials, such as those used in sorption thermochemical heat storage systems, are difficult to determine. It is difficult to enter these thermal parameters into programs that simulate the working and operation scenarios of thermochemical heat storage devices because of the lack of precision in measurement and contradictory findings. For this reason, in this work, different methods have been applied and compared in order to improve the accuracy of the measurement. In this study, we focused on the working pair “zeolite 13X–water” under atmospheric pressure. The temperature range being investigated corresponds to the operating conditions of a low-grade adsorptive heat storage device, i.e. 20 – 95 °C.

Material and methods

The material used in this study is a commercial zeolite 13X “Zeolum F-9 14-20#” from Tosoh Europe B.V., Amsterdam, Netherlands. The diameter of the spherical particles (beads) is in the range of 0.85 mm–1.18 mm. The textural properties of the material were investigated by N_2

adsorption experiments. The isotherm is of type I at low relative pressure, which is characteristic of a microporous material. The porous volume is $0.28 \text{ cm}^3 \text{ g}^{-1}$.

Three thermo-physical properties are investigated in this study: the apparent thermal conductivity of the material bed λ ($\text{W m}^{-1} \text{ K}^{-1}$), the specific heat C_p ($\text{J kg}^{-1} \text{ K}^{-1}$) and the apparent density of the material ρ (kg m^{-3}).

Density

The apparent density of the material bed (bulk density) is measured under a controlled atmosphere (T and relative humidity, RH). Several samples of material (150.00 g of zeolite) are taken at room conditions, and the volume is measured in a 250 mL graduated cylinder. The samples are dehydrated in an oven at $300 \text{ }^\circ\text{C}$ for 3 days and then rehydrated at the desired moisture content. In a glove box, the samples are weighted again. To take into account the influence of graduated cylinder filling, the results are presented according to the chosen samples.

To estimate the void fraction (inter-granular porosity), the intrinsic density of the material is calculated by weighing and measuring 4-5 beads with a microbalance and an electronic slide gauge (repeated several times).

Thermal conductivity

The estimation of the material's thermal properties required the use of several techniques owing to intricate balances between temperature, humidity, and reaction heat of sorption. The apparent thermal conductivity of the material was first investigated by using a transient line source (hot-wire method). The apparatus is a TLS-100 (Thermtest Inc., Fredericton, NB, Canada), with a 100 mm long probe. The diameter of the tested sample is greater than 50 mm and its depth is 120 mm, in agreement with the manufacturer's recommendations. The probe heats the sample at constant

power and records its temperature. The apparent thermal conductivity is calculated assuming one-dimensional heat transfer in an infinite solid.

Second, a custom guarded hot plate setup (Delta Lab ET 100, Carcassonne, France) is also used to measure the apparent thermal conductivity of the bed. The sample dimensions are $300 \times 250 \times 24$ mm (length \times width \times depth). It is placed between two aluminium plates (up and down). The bottom plate is placed on 96 mm of expanded polystyrene (λ_{ps}) and heated by joule effect (P_0) to the required (constant) temperature. The two plates are instrumented with 3 thermocouples each (average temperature: T_b and T_t). Once the steady state is reached, the thermal conductivity is calculated according to one-dimensional Fourier's law, taking into account heat transfer in the insulation (equation 1).

$$\lambda = \frac{P_0 \cdot d}{(T_b - T_t)} - \lambda_{ps} \frac{(T_b - T_o)}{4(T_b - T_t)} \quad (1)$$

A transient plane source technique is also used to measure the thermal conductivity of the material. It consists of a Hot Disk M1 thermal constants analyser (Hot Disk AB, Gothenburg, Sweden) with a "Kapton 8563 F1" sensor (disc radius: $a = 9.868$ mm). It also provides the estimation of the thermal diffusivity ($\alpha = \frac{\lambda}{\rho C_p}$, $\text{m}^2 \text{s}^{-1}$), the thermal effusivity ($E = (\rho C_p \lambda)^{\frac{1}{2}}$, $\text{J K}^{-1} \text{m}^{-2} \text{s}^{-0.5}$), and the specific heat (ρC_p , in $\text{J m}^{-3} \text{K}^{-1}$). The sample is in a cubic box (thickness: 60 mm, side length: 70 mm). The probe is horizontally placed in the middle of the bed and heats the material at constant power P_0 (W) and records its temperature increase ΔT for a few minutes.

Heat capacity

As previously described, the heat capacity can be deduced from experiments with the transient plane source ("hot disk"). These tests can be conducted only at room temperature and in a glove

box to avoid material moisture variation. To investigate the effects of both “temperature” and “water content”, a two-in-one thermo-gravimetric and differential scanning calorimetry analyzer (Setaram Sensys evo TG-DSC, Kep Technologies, Caluire, France) is used.

A typical sample is constituted of approximately 10 mg of material (10 beads) contained in an aluminium crucible. It is suspended on a microscale along with another empty crucible. To control their temperature, both crucibles are enclosed in furnaces. The differential heat-flow signal is recorded thanks to a Calvet sensor. The atmosphere in the chamber is a flow of synthetic air, which mass flow, temperature, and humidity are controlled by a humidity generator (Setaram Wetsys, Kep Technologies, Caluire, France).

First, the sample is dehydrated at 300 °C with synthetic air (30 mL min⁻¹ airflow rate pulsed by the humidity controller) for 8 h. The duration of 8 h allows to reach mass stability, such as $dm/dt < 0.006 \text{ \% min}^{-1}$, following the stability criterion employed by Son et al. [38]. The sample is then cooled and rehydrated to the required temperature and moisture by adjusting the air humidity.

Following its pre-treatment, the sample is heated up to 110 °C at a constant heating rate while maintaining the mass of the sample constant. For this, the air humidity is continuously adjusted.

Heat capacity is continuously calculated using equation 2:

$$Cp = \left[\left(\frac{dq}{dt} \right)_{sample} - \left(\frac{dq}{dt} \right)_{blank} \right] \cdot \frac{1}{m_0 \cdot \frac{dT}{dt}} \quad (2)$$

With $\left(\frac{dq}{dt} \right)_{sample}$, $\left(\frac{dq}{dt} \right)_{blank}$ the DSC signal during the sample and the blank tests, respectively.

m_0 is the mass of the sample (maintained constant) and $\frac{dT}{dt}$ the heating rate.

The quality of experimental results (y_i) was examined using three criteria (range, mean absolute deviation, and standard deviation) and their respective relative values (divided by average value \bar{y}):

Range: $R = \max(y_i) - \min(y_i)$

Mean absolute deviation $MAD = \frac{1}{N} \sum_1^N |y_i - \bar{y}|$

Standard deviation $SD = \sqrt{\frac{\sum_1^N (y_i - \bar{y})^2}{N}}$

Results and discussion

Preliminary tests

Data available in the literature on the thermo-physical properties of reactive and hygroscopic materials is uncertain and even minimal for zeolite 13X. Under these conditions, the first step is to investigate the different characterization techniques in order to assess the feasibility, reliability, and quality of measurements. For this, the thermo-physical properties of zeolite 13X were investigated with different techniques at room humidity and temperature conditions. The thermo-physical properties of the material in equilibrium with air at room temperature and humidity are shown in Table 2.

Table 2 Preliminary tests performed with the material in equilibrium (thermal and water balances) with the ambience

	value	tests	R	$R(\%)$	MAD	$MAD(\%)$	SD	$SD(\%)$
$w / \text{kg kg}^{-1}$	0.193	8	0.027	13.9	0.014	7.0	0.015	8
$\rho / \text{Kg M}^{-3}$	794	38	78	9.9	16	2.1	20.8	3
$\lambda / \text{mW m}^{-1} \text{K}^{-1}$ (Hot Wire)	94.5	8	6	6.3	1	1.5	1.7	2
$\lambda / \text{mW m}^{-1} \text{K}^{-1}$ (Hot disk)	120.8	22	33	27.6	23	19.1	7.3	7
$\lambda / \text{mW m}^{-1} \text{K}^{-1}$ (Hot Plate)	93.9	9	23	24.4	6	6.8	7.3	7

$E/W \text{ m}^{-2} \text{ K}^{-1} \text{ s}^{-0.5}$ (Hot disk)	337	22	31	9.1	7.9	1.9	7.7	2
$10^7 D / \text{m}^2 \text{ s}^{-1}$ (Hot disk)	1.29	22	0.70	54.2	0.13	9.7	1.63	13
$\rho C_P / \text{mJ m}^{-3} \text{ K}^{-1}$ (Hot disk)	0.94	22	0.28	29.8	0.13	14.0	0.07	8
$C_p / \text{J kg}^{-1} \text{ K}^{-1}$ (DSC) ($T = 60$ to 95°C)	1369	1						

First, we can observe a difference in the thermal conductivity values obtained by the hot disk and the other experiments (around 30%) and a greater dispersion of experimental values ($MAD > 19\%$). The same holds true for the specific heat capacity ($MAD \approx 14\%$). Moreover, the heat capacity is low in comparison with the literature and the results obtained by thermo-gravimetric investigations.

According to the theory, the thermal conductivity and the specific heat are simultaneously estimated by fitting the experimental temperature of the sensor with equation 3.

$$\Delta T = \frac{P_0}{\pi^2 \lambda r} \int_0^\tau \frac{d\sigma}{\sigma^2} \int_0^1 v dv \int_0^1 \exp\left(\frac{-(u^2+v^2)}{4\sigma^2}\right) I_0\left(\frac{uv}{2\sigma^2}\right) u du \quad (3)$$

P_0 is the power input, I_0 represents the 0 order modified Bessel functions and $\tau = \sqrt{\frac{Dt}{r^2}}$. With t the time measured from the start of the experiment, D is the thermal diffusivity of the material and r is the radius of the hot disk.

In practice, this equation is not used in the calculation, because of its complexity [33,39,40]. Indeed, after a comparison between the calculations carried out by the software and our calculations, it was observed that the software used the solution of a one-dimensional heat transfer problem. The system (material and heat source) is assumed to be a 1D half-space unsteady problem subjected to

a constant heat flux. The solution to this problem leads to a temperature profile in the material bed as follows (eq. 4):

$$T(x, t) = T(t = 0) + \frac{P_0}{\lambda S} \sqrt{Dt} \left[\frac{1}{\sqrt{\pi}} e^{-\frac{x^2}{4Dt}} - \frac{x}{2\sqrt{Dt}} \operatorname{erfc} \left(\frac{x}{2\sqrt{at}} \right) \right] \quad (4)$$

Starting from this equation the sensor temperature is ($x = 0$):

$$T(x = 0, t) = T(t = 0) + \frac{P_0}{\lambda S} \sqrt{Dt} \left[\frac{1}{\sqrt{\pi}} \right] \quad (5)$$

The thermo-physical properties are estimated first by fitting the experimental sensor temperature with a function of the square root of time. The slope of the linear curve of $T(t)$ versus \sqrt{t} is directly proportional to the material effusivity $E = \sqrt{\rho C_p \lambda}$. The study of the different temperature profiles shows good linearity and explains that the estimation of E is given with low dispersion.

Second, the thermal conductivity is estimated by minimizing a quadratic criterion between the sensor temperature (experimental) and equation 3 after significant simplifications. For this, the three integrals are substituted by a polynomial function of τ (the polynomial coefficients are previously pre-calculated from equation 3).

For this material, the obtained thermal conductivity is different from the ones measured with hot-wire and hot plate techniques. Moreover, we observe a significant dispersion of the results.

The same conclusions are observed for specific heat and thermal diffusivity because they are deduced from calculations of effusivity and thermal conductivity.

From these results and observations, we can conclude that the transient plane source technique is not well suited for measuring the thermal conductivity and heat capacity of this material. Consequently, the thermal diffusivity is affected by a large uncertainty. Only the material effusivity can be estimated accurately.

Starting from these preliminary results, the material properties were investigated by using a hot wire for thermal conductivity, TG-DSC for specific heat, and a hot disk for effusivity.

Thermo-physical properties of zeolite 13X

Material density was measured at room temperature for different moisture contents according to the protocol detailed in the previous section. This methodology was applied owing to the influence of material placement operations. The results are shown in Fig. 1.

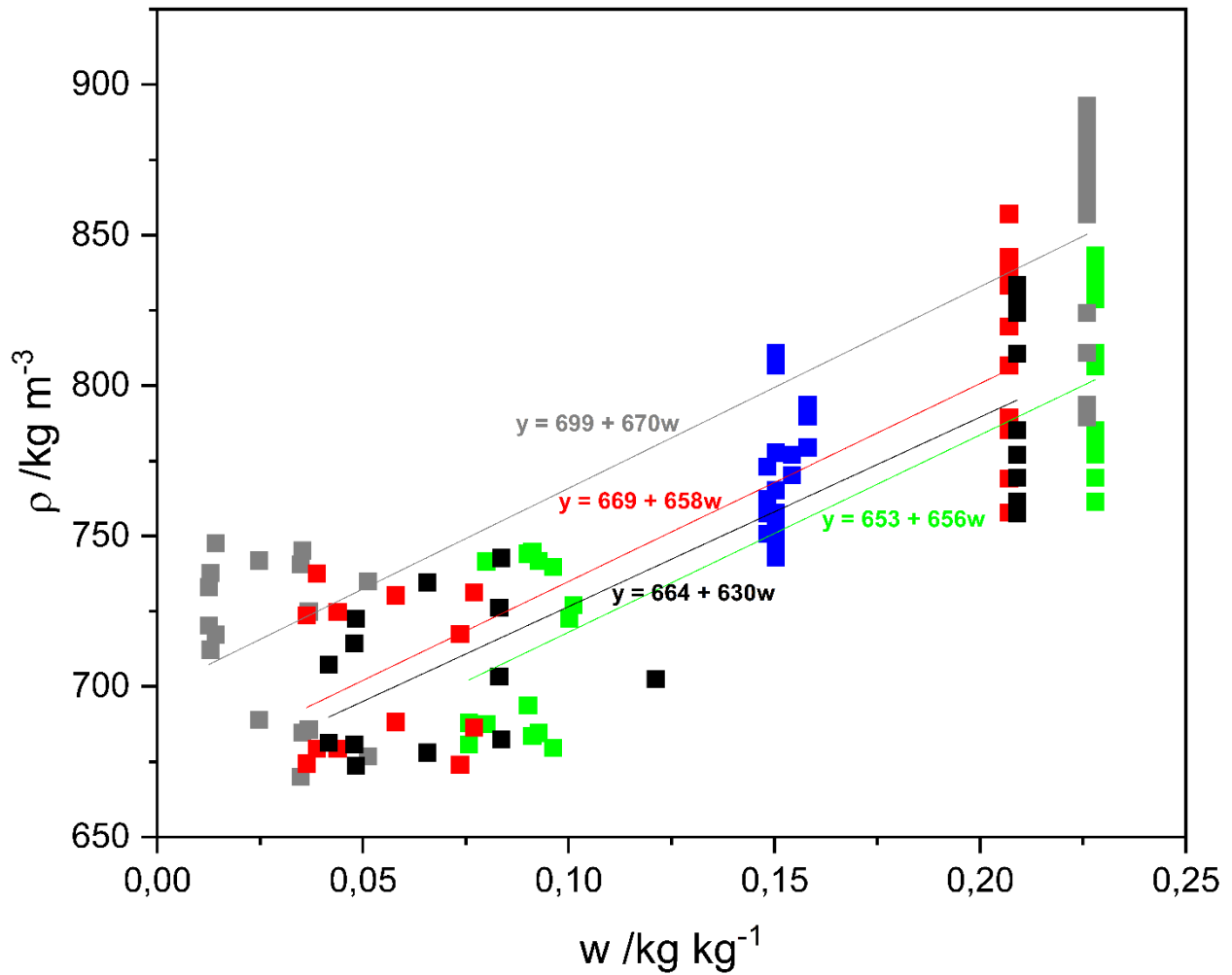


Fig. 1 Material apparent density as a function of water content

As expected, the bulk density of zeolite 13X is linearly proportional to the water mass fraction. The difference in Y-intercept is due to the difference in material placement in the column. This difference is about 50 kg m^{-3} . The density of the dried material is about $\rho_0 = 662 \text{ kg m}^{-3}$. The best fitted equations for the studied samples are consistent with the theory, i.e. $\rho = \rho_0 (1 + w)$. The intrinsic density of the material is 1160 kg m^{-3} at $w = 0.235 \text{ kg kg}^{-1}$. The void fraction is estimated to be in the range of 26 – 32 %. Additional tests at different temperatures (up to $90 \text{ }^\circ\text{C}$) reveal the same behavior. The bulk density does not appear to be dependent on temperature, but only on filling ways.

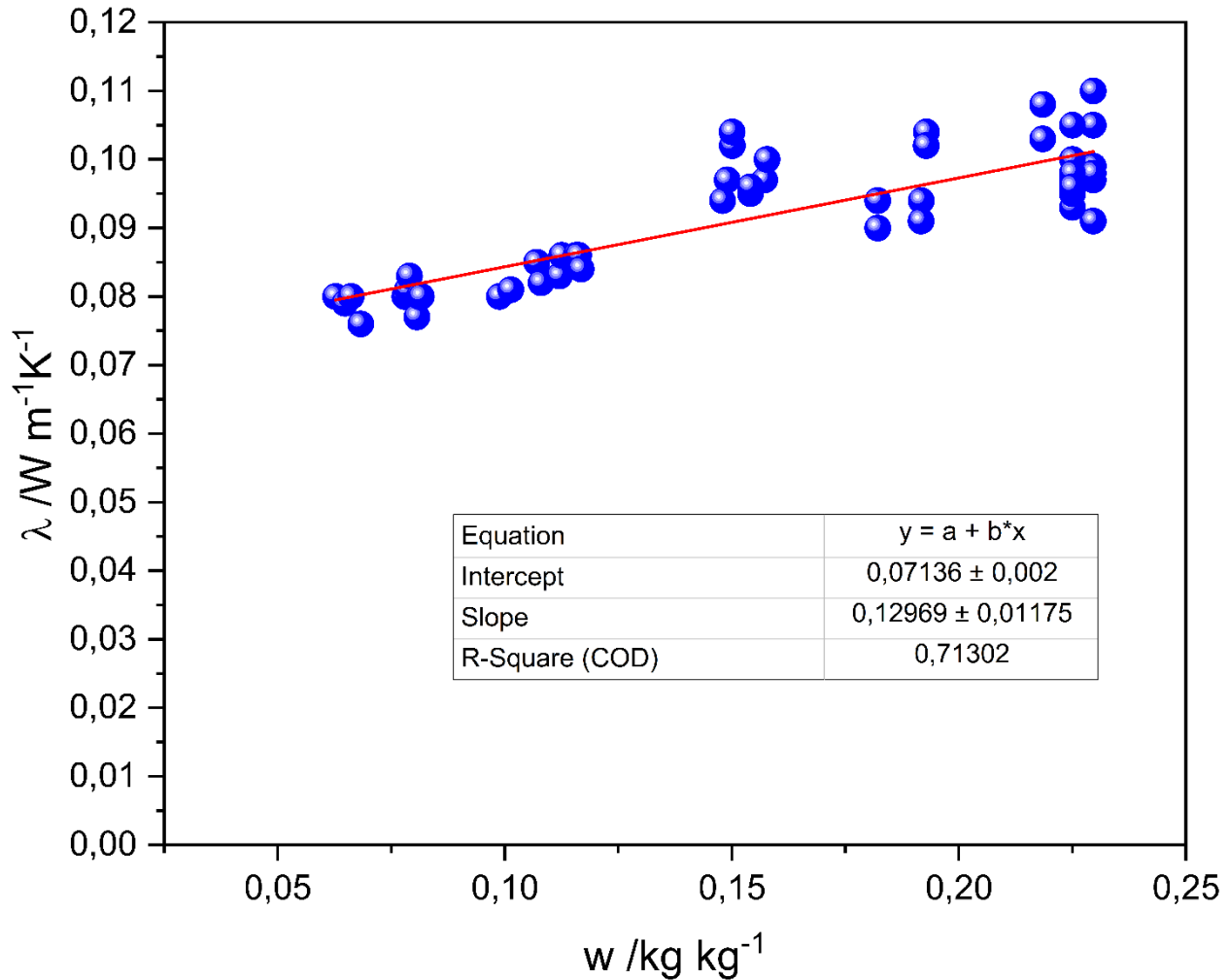


Fig. 2 Apparent thermal conductivity of a zeolite 13X bed versus water content

The apparent thermal conductivity of the zeolite bed of around 1 mm diameter beads is shown in Fig. 2. It is a linear function of the inner moisture content.

The thermal conductivity is low and can be explained by the important void fraction (around 30%) and the porous volume that represents two thirds of the volume. The presence of adsorbed water in the pores improves the conductive heat transfer inside the beads. These results are in good agreement with the results of A. Aittomaki and A. Aula [36]. The thermal conductivity of a dry bed of zeolite 13X (diameter of particles 2-3 mm) is $0.076 \text{ W m}^{-1} \text{ K}^{-1}$. The dependence on

temperature of the bulk thermal conductivity is very complicated to investigate owing to the relationship between temperature and water content. Additional tests performed on a guarded hot plate (up to 50 °C) do not show a change with temperature. This would be expected since air (void fraction) is mainly responsible for the low thermal conductivity. Indeed, the thermal conductivity of dry air slightly increases with temperature (from 26 to 31 mW m⁻¹ K⁻¹ in the range of 20–90 °C).

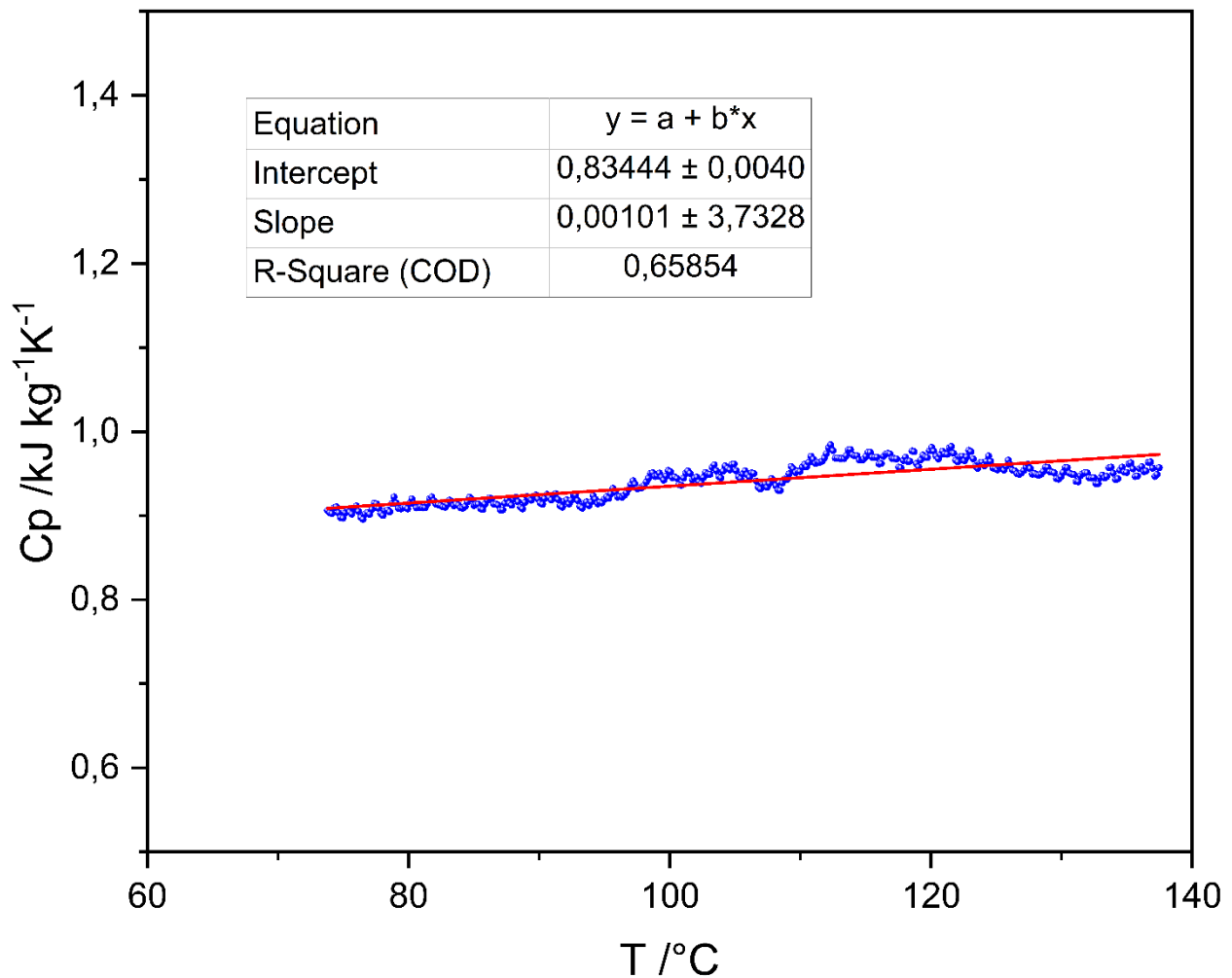


Fig. 3 specific heat of dried zeolite 13X versus temperature

The specific heat of the material is estimated by using a differential scanning calorimetry analyzer.

The experiments were carried out at temperatures ranging from 65 to 140 °C for the dried material

and from 60 to 90 °C for the material at different water contents. Figure 3 shows the specific heat of the dried material. A slight increase in specific heat with temperature is observed, but in the range of 70 – 95 °C, this value is constant at 913 J kg⁻¹ K⁻¹. This result is indeed quite different from the specific heat obtained by Simonot-Grange [24] for anhydrous zeolite 13X.

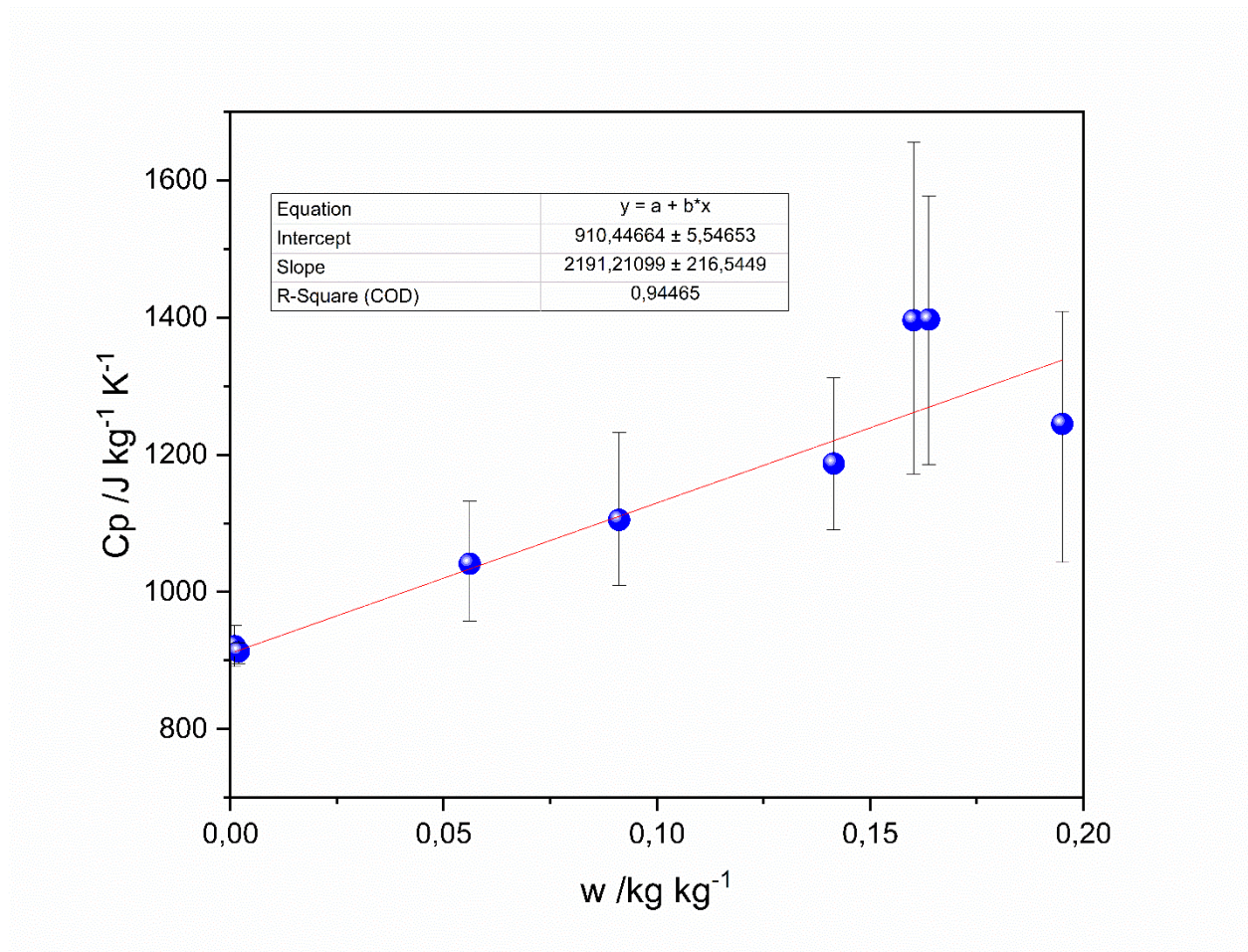


Fig. 4 specific heat of zeolite 13X for different water contents

The same experiments are repeated for different water contents. For this, the air humidity is controlled to have a constant mass of material. Figure 4 shows the specific heat of the material at different moisture content. The specific heat seems to vary linearly with water content. Results show that the experimental error increases with the water content due to the difficulty of controlling a constant mass of material.

From the linear approximation, the specific heat of the dried material $Cp(db)$ is $910 \text{ J kg}^{-1} \text{ K}^{-1}$ (max = 916, min = $905 \text{ J kg}^{-1} \text{ K}^{-1}$), which is close to $913 \text{ J kg}^{-1} \text{ K}^{-1}$ (obtained for dried material). The slope is $2191 \pm 217 \text{ J kg}^{-1} \text{ K}^{-1}$.

For this material type, many authors assumed a linear variation with water content. A linear rule of mixing (equation 7) can be applied to calculate the specific heat of the hydrated material.

$$Cp = Cp(db) + w[Cp(H_2O) - Cp(db)] \quad (7)$$

With this assumption, the specific heat capacity of water in the material is about $3100 \text{ J kg}^{-1} \text{ K}^{-1}$ (max = 3323, min = $2878 \text{ J kg}^{-1} \text{ K}^{-1}$).

This result is in good agreement with data available in the literature [25]. Indeed, Hirasawa *et al.* conclude that the specific heat of adsorbed water is about 3000 to $5000 \text{ J kg}^{-1} \text{ K}^{-1}$. This value is an intermediate value between the liquid and vapor specific heats of water (i.e. 4190 and $1830 \text{ J kg}^{-1} \text{ K}^{-1}$, respectively).

In order to verify the relevance of the properties estimations, calculated effusivity values are compared to results from hot disk experiments.

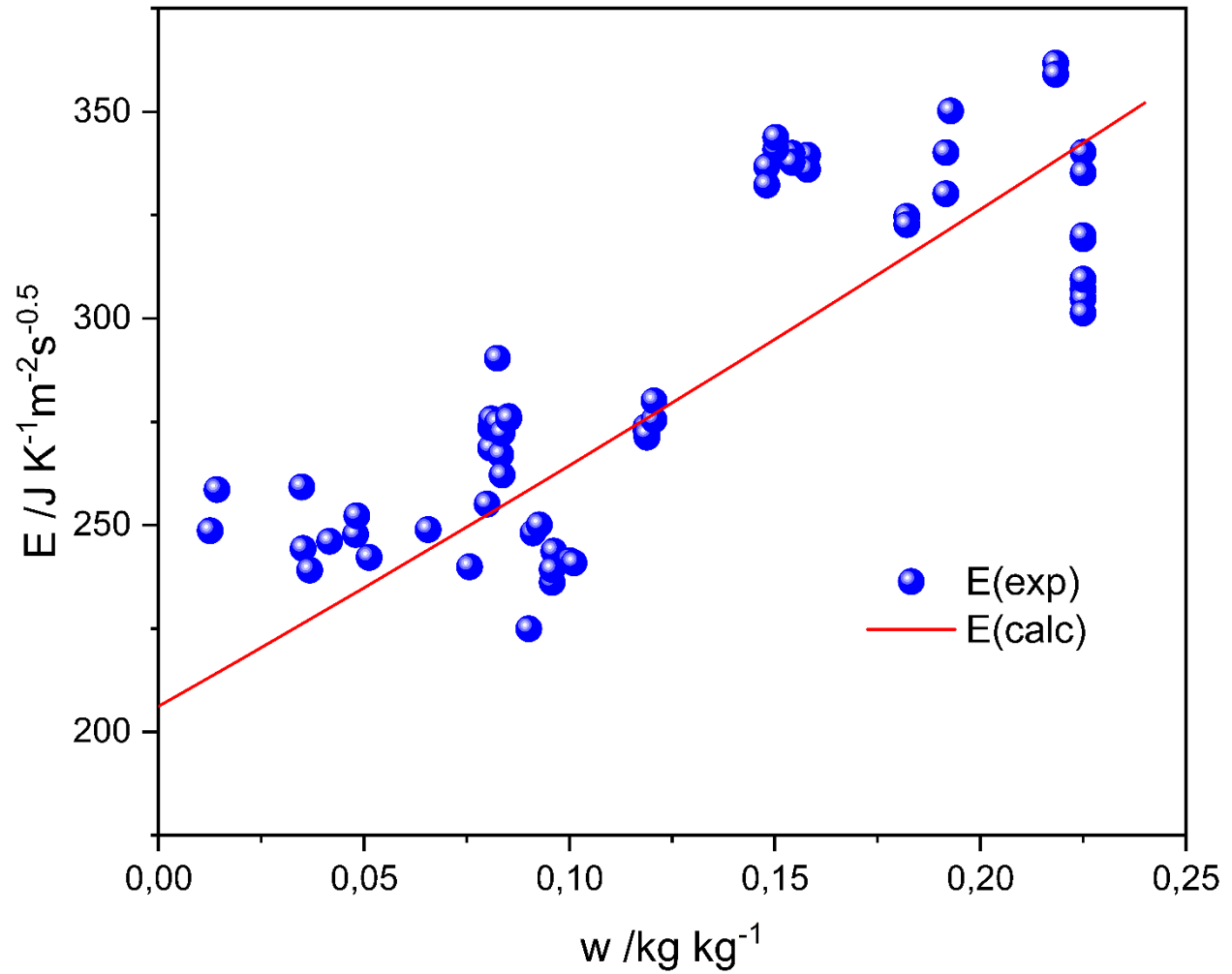


Fig. 5 material effusivity (experimental and calculated) as a function of water content

Figure 5 shows the experimental effusivity values (from hot disk experiments) and the calculated ones by using equation 8 as follows:

$$E = [662(1 + w)(71 + 130w)10^{-3}(904 + 2391w)]^{\frac{1}{2}} \quad (8)$$

Calculated and experimental results are in good agreement, validating the applied methodology.

Conclusion

A precise estimation of the thermo-physical properties of adsorbent and reactive materials is a necessary and inevitable step for the development of heat storage systems. In this work, different techniques were used and compared to improve the measurement accuracy. In particular, results show that the transient hot disk method is not suitable for estimating the thermal conductivity and the heat capacity of this type of material. There was a significant difference in thermal conductivity (approximately 30%) between the hot disc studies and the other methods, as well as a greater dispersion of the experimental results (MAD > 19%). The same was discovered for specific heat capacity (MAD \approx 14%). Nevertheless, this technique enables a good estimation of the thermal effusivity. Thermal conductivity and heat capacity were investigated by hot wire and TG-DSC, respectively. There was a little rise in specific heat with temperature, although this value remains constant at $913 \text{ J kg}^{-1} \text{ K}^{-1}$ between 70 and 95 °C. Experimental and calculated thermal effusivity values from independent characterization validate the applied methodology. These results allow to obtain the thermo-physical properties of a reactive and hygroscopic material as a function of temperature and water content in a larger range of operating conditions than those reported up to now in the literature. These data are required as key input data for simulating thermochemical heat storage operations.

References

1. Uddin K, Amirul Islam M, Mitra S, Lee J, Thu K, Saha BB, et al. Specific heat capacities of carbon-based adsorbents for adsorption heat pump application. *Appl Therm Eng* [Internet]. 2018;129:117–26. Available from: <https://linkinghub.elsevier.com/retrieve/pii/S1359431117345726>
2. Qiu L, Murashov V, White MA. Zeolite 4A: heat capacity and thermodynamic properties. *Solid State Sci* [Internet]. 2000;2:841–6. Available from: <https://linkinghub.elsevier.com/retrieve/pii/S129325580001102X>
3. Hauer A. Sorption theory for thermal energy storage. *Therm Energy Storage Sustain Energy Consum* [Internet]. Dordrecht: Springer Netherlands; 2007. p. 393–408. Available from: http://link.springer.com/10.1007/978-1-4020-5290-3_24
4. Gordeeva LG, Aristov YI. Adsorptive heat storage and amplification: New cycles and adsorbents. *Energy* [Internet]. 2019;167:440–53. Available from: <https://linkinghub.elsevier.com/retrieve/pii/S0360544218321285>
5. Nagel T, Beckert S, Lehmann C, Gläser R, Kolditz O. Multi-physical continuum models of thermochemical heat storage and transformation in porous media and powder beds—A review. *Appl Energy* [Internet]. 2016;178:323–45. Available from: <https://linkinghub.elsevier.com/retrieve/pii/S0306261916308261>
6. Yu N, Wang RZ, Wang LW. Sorption thermal storage for solar energy. *Prog Energy Combust Sci* [Internet]. 2013;39:489–514. Available from: <https://linkinghub.elsevier.com/retrieve/pii/S0360128513000270>
7. Lehmann C, Beckert S, Nonnen T, Gläser R, Kolditz O, Nagel T. Water loading lift and heat storage density prediction of adsorption heat storage systems using Dubinin-Polanyi theory—Comparison with experimental results. *Appl Energy* [Internet]. 2017;207:274–82. Available from: <https://linkinghub.elsevier.com/retrieve/pii/S0306261917308735>
8. Ye W-B, Guo H-J, Huang S-M, Hong Y-X. Research on melting and solidification processes for enhanced double tubes with constant wall temperature/wall heat flux. *Heat Transf Res* [Internet]. 2018;47:583–99. Available from: <https://onlinelibrary.wiley.com/doi/10.1002/htj.21328>
9. Aristov YI. Adsorptive transformation of heat: Principles of construction of adsorbents database. *Appl Therm Eng* [Internet]. 2012;42:18–24. Available from: <https://linkinghub.elsevier.com/retrieve/pii/S1359431111001049>
10. (IUPAC) TIU of P and AC. Isosteric enthalpy of adsorption. *Compend Chem Terminol* [Internet]. 2014. p. 790–3. Available from: <https://goldbook.iupac.org/files/pdf/goldbook.pdf>
11. Azahar FHM, Mitra S, Yabushita A, Harata A, Saha BB, Thu K. Improved model for the isosteric heat of adsorption and impacts on the performance of heat pump cycles. *Appl Therm Eng* [Internet].

- 2018;143:688–700. Available from: <https://linkinghub.elsevier.com/retrieve/pii/S1359431118323950>
12. Brancato V, Frazzica A. Experimental Methods for the Characterization of Materials for Sorption Storage. 2019. p. 119–37. Available from: http://link.springer.com/10.1007/978-3-319-96640-3_9
 13. Semprini S, Asenbeck S, Kerskes H, Drück H. Experimental and numerical investigations of an adsorption water-zeolite heat storage for refrigeration applications. *Energy Procedia* [Internet]. 2017;135:513–21. Available from: <https://linkinghub.elsevier.com/retrieve/pii/S1876610217345952>
 14. Li W, Klemeš JJ, Wang Q, Zeng M. Performance analysis of consolidated sorbent based closed thermochemical energy storage reactor for environmental sustainability. *J Clean Prod* [Internet]. 2020;265:121821. Available from: <https://linkinghub.elsevier.com/retrieve/pii/S0959652620318680>
 15. Dawoud B, Sohel MI, Freni A, Vasta S, Restuccia G. On the effective thermal conductivity of wetted zeolite under the working conditions of an adsorption chiller. *Appl Therm Eng* [Internet]. 2011;31:2241–6. Available from: <https://linkinghub.elsevier.com/retrieve/pii/S1359431111001487>
 16. Freni A, Tokarev M., Restuccia G, Okunev A., Aristov Y. Thermal conductivity of selective water sorbents under the working conditions of a sorption chiller. *Appl Therm Eng* [Internet]. 2002;22:1631–42. Available from: <https://linkinghub.elsevier.com/retrieve/pii/S1359431102000765>
 17. Rocky KA, Islam MA, Pal A, Ghosh S, Thu K, Nasruddin, et al. Experimental investigation of the specific heat capacity of parent materials and composite adsorbents for adsorption heat pumps. *Appl Therm Eng* [Internet]. 2020;164:114431. Available from: <https://linkinghub.elsevier.com/retrieve/pii/S1359431119337135>
 18. Tanashev YY, Krainov A V., Aristov YI. Thermal conductivity of composite sorbents “salt in porous matrix” for heat storage and transformation. *Appl Therm Eng* [Internet]. 2013;61:401–7. Available from: <https://linkinghub.elsevier.com/retrieve/pii/S1359431113006030>
 19. Liu ZY, Cacciola G, Restuccia G, Giordano N. Fast simple and accurate measurement of zeolite thermal conductivity. *Zeolites* [Internet]. 1990;10:565–70. Available from: <https://linkinghub.elsevier.com/retrieve/pii/S0144244905803136>
 20. Bird JE, Humphries TD, Paskevicius M, Poupin L, Buckley CE. Thermal properties of thermochemical heat storage materials. *Phys Chem Chem Phys* [Internet]. 2020;22:4617–25. Available from: <http://xlink.rsc.org/?DOI=C9CP05940G>
 21. Vučelić V, Vučelić D. The heat capacity of water near solid surfaces. *Chem Phys Lett* [Internet]. 1983;102:371–4. Available from: <https://linkinghub.elsevier.com/retrieve/pii/0009261483870584>
 22. Schwamberger V, Schmidt FP. Estimating the Heat Capacity of the Adsorbate–Adsorbent System from Adsorption Equilibria Regarding Thermodynamic Consistency. *Ind Eng Chem Res* [Internet]. 2013;52:16958–65. Available from: <https://pubs.acs.org/doi/10.1021/ie4011832>
 23. Berezin GI, Kiselev A V., Sinitsyn VA. Heat capacity of the H₂O/KNaX zeolite adsorption system. *J*

Chem Soc Faraday Trans 1 Phys Chem Condens Phases [Internet]. 1973;69:614. Available from: <http://xlink.rsc.org/?DOI=f19736900614>

24. Simonot-Grange M-H, Belhamidi-El Hannouni F, Bracieux-Bouillot O. Propriétés physico-chimiques de l'eau adsorbée dans les zeolithes 13X et 4A. II. Capacités thermiques de l'eau adsorbée, du système zeolithe—eau et de la zeolithe anhydre. *Thermochim Acta* [Internet]. 1986;101:217–30. Available from: <https://linkinghub.elsevier.com/retrieve/pii/0040603186800569>

25. Hirasawa Y, Urakami W. Study on Specific Heat of Water Adsorbed in Zeolite Using DSC. *Int J Thermophys* [Internet]. 2010;31:2004–9. Available from: <http://link.springer.com/10.1007/s10765-010-0841-6>

26. Lu X, Wang Y, Estel L, Kumar N, Grénman H, Leveneur S. Evolution of Specific Heat Capacity with Temperature for Typical Supports Used for Heterogeneous Catalysts. *Processes* [Internet]. 2020;8:911. Available from: <https://www.mdpi.com/2227-9717/8/8/911>

27. Mette B, Kerskes H, Drück H, Müller-Steinhagen H. Experimental and numerical investigations on the water vapor adsorption isotherms and kinetics of binderless zeolite 13X. *Int J Heat Mass Transf* [Internet]. 2014;71:555–61. Available from: <https://linkinghub.elsevier.com/retrieve/pii/S001793101301106X>

28. Chakraborty A, Saha BB, Koyama S, Ng KC. Specific heat capacity of a single component adsorbent-adsorbate system. *Appl Phys Lett* [Internet]. 2007;90:171902. Available from: <http://aip.scitation.org/doi/10.1063/1.2731438>

29. Tatlier M, Tantekin-Ersolmaz B, Erdem-Şenatalar A. A novel approach to enhance heat and mass transfer in adsorption heat pumps using the zeolite–water pair. *Microporous Mesoporous Mater* [Internet]. 1999;27:1–10. Available from: <https://linkinghub.elsevier.com/retrieve/pii/S1387181198001747>

30. Griesinger A, Spindler K, Hahne E. Measurements and theoretical modelling of the effective thermal conductivity of zeolites. *Int J Heat Mass Transf* [Internet]. 1999;42:4363–74. Available from: <https://linkinghub.elsevier.com/retrieve/pii/S0017931099000964>

31. Hu P, Yao J-J, Chen Z-S. Analysis for composite zeolite/foam aluminum–water mass recovery adsorption refrigeration system driven by engine exhaust heat. *Energy Convers Manag* [Internet]. 2009;50:255–61. Available from: <https://linkinghub.elsevier.com/retrieve/pii/S0196890408003701>

32. Log T, Gustafsson SE. Transient plane source (TPS) technique for measuring thermal transport properties of building materials. *Fire Mater* [Internet]. 1995;19:43–9. Available from: <https://onlinelibrary.wiley.com/doi/10.1002/fam.810190107>

33. KRAPEZ J-C. Mesure de l'effusivité thermique - Méthodes par contact [Internet]. *Tech. d'analyse*. 2007 Mar. Available from: <https://www.techniques-ingenieur.fr/doi/10.51257/a/v1/r2958>

34. Pinheiro JM, Salústio S, Valente AA, Silva CM. Adsorption heat pump optimization by experimental design and response surface methodology. *Appl Therm Eng* [Internet]. 2018;138:849–60. Available from:

<https://linkinghub.elsevier.com/retrieve/pii/S1359431117351219>

35. Zheng Q, Kaur S, Dames C, Prasher RS. Analysis and improvement of the hot disk transient plane source method for low thermal conductivity materials. *Int J Heat Mass Transf* [Internet]. 2020;151:119331. Available from: <https://linkinghub.elsevier.com/retrieve/pii/S0017931019362234>
36. Aittomäki A, Aula A. Determination of effective thermal conductivity of adsorbent bed using measured temperature profiles. *Int Commun Heat Mass Transf* [Internet]. 1991;18:681–90. Available from: <https://linkinghub.elsevier.com/retrieve/pii/073519339190080N>
37. Wang L, Zhu D, Tan Y. Heat Transfer Enhancement on the Adsorber of Adsorption Heat Pump. *Adsorption* [Internet]. 1999;5:279–86. Available from: <https://doi.org/10.1023/A:1008964013879>
38. Son KN, Richardson T-MJ, Cmarik GE. Equilibrium Adsorption Isotherms for H₂O on Zeolite 13X. *J Chem Eng Data* [Internet]. 2019;64:1063–71. Available from: <https://pubs.acs.org/doi/10.1021/acs.jced.8b00961>
39. Malinarič S. Contribution to the Transient Plane Source Method for Measuring Thermophysical Properties of Solids. *Int J Thermophys* [Internet]. 2013;34:1953–61. Available from: <http://link.springer.com/10.1007/s10765-013-1502-3>
40. Malinarič S, Dieška P. Concentric Circular Strips Model of the Transient Plane Source-Sensor. *Int J Thermophys* [Internet]. 2015;36:692–700. Available from: <http://link.springer.com/10.1007/s10765-015-1848-9>